

The 2013 outburst of a transient very faint X-ray binary, 23” from Sgr A*

E. W. Koch^{1,2}, A. Bahramian¹, C. O. Heinke¹, K. Mori³, N. Rea^{4,5}, N. Degenaar^{6,7}, D. Haggard^{8,9}, R. Wijnands⁴, G. Ponti¹⁰, J. M. Miller⁶, F. Yusef-Zadeh⁸, F. Dufour¹¹, W. D. Cotton¹², F. K. Baganoff¹³, M. T. Reynolds⁶

¹ Dept. of Physics, University of Alberta, CCIS 4-183, Edmonton, AB T6G 2E1, Canada; bahramia@ualberta.ca, heinke@ualberta.ca

² Unit 5, Physics Program, UBC-Okanagan, 3333 University Way, Kelowna, BC V1V 1V7, Canada; koch.eric.w@gmail.com

³ Columbia Astrophysics Laboratory, Columbia University, New York, NY 10027 USA

⁴ Astronomical Institute "Anton Pannekoek," University of Amsterdam, Postbus 94249, NL-1090 GE Amsterdam, The Netherlands

⁵ Institute of Space Sciences (CSIC-IEEC), Campus UAB, Torre C5, 2a planta, E-08193 Barcelona, Spain

⁶ Department of Astronomy, University of Michigan, 500 Church Street, Ann Arbor, MI 48109, USA

⁷ Hubble Fellow

⁸ CIERA and Physics & Astronomy Dept., Northwestern University, 2145 Sheridan Road, Evanston, IL 60208, USA

⁹ CIERA Fellow

¹⁰ School of Physics and Astronomy, University of Southampton, Highfield, Southampton SO17 1BJ, UK

¹¹ Department of Physics, McGill University, 3600 rue University, Montreal, QC H3A 2T8, Canada

¹² National Radio Astronomy Observatory, 520 Edgemont Road, Charlottesville, VA 22903-2475, USA

¹³ Kavli Institute for Astrophysics and Space Research, Massachusetts Institute of Technology, Cambridge, MA 02139, USA

ABSTRACT

We report observations using the Swift/XRT, NuSTAR, and Chandra X-ray telescopes of the transient X-ray source CXOGC J174540.0-290005, during its 2013 outburst. Due to its location in the field of multiple observing campaigns targeting Sgr A*, this is one of the best-studied outbursts of a very faint X-ray binary (VFXB; peak $L_X < 10^{36}$ erg/s) yet recorded, with detections in 173 ks of X-ray observations over 50 days. VFXBs are of particular interest, due to their unusually low outburst luminosities and time-averaged mass transfer rates, which are hard to explain within standard accretion physics and binary evolution. The 2013 outburst of CXOGC J174540.0-290005 peaked at $L_X(2-10\text{ keV})=5.0 \times 10^{35}$ erg/s, and all data above 10^{34} ergs/s were well-fit by an absorbed power-law of photon index ~ 1.7 , extending from 2 keV out to $\gtrsim 70$ keV. We discuss the implications of these observations for the accretion state of CXOGC J174540.0-290005.

Key words: accretion, accretion discs – (stars:) binaries – X-rays: binaries – X-rays: individual: CXOGC J174540.0-290005

1 INTRODUCTION

The majority of low-mass X-ray binaries (LMXBs; neutron stars (NSs) or black holes accreting from low-mass companion stars) are transient systems, showing brief outbursts of X-ray luminosity $10^3 - 10^9$ times higher than during quiescence. This transient behaviour is generally understood to be due to thermal-viscous accretion disk instabilities (e.g. Smak 1984; King et al. 1998; Lasota 2001; Coriat et al. 2012). As programs to identify new outbursts from LMXBs in our Galaxy have become more sophisticated, they have identified progressively fainter outbursts. Monitoring of the Galactic Centre region has uncovered significant numbers of transient outbursts exhibiting peak X-ray luminosities

of $10^{34} - 10^{35}$ ergs/s, using XMM-Newton (Sakano et al. 2005), Chandra (Muno et al. 2005), XMM and Chandra (Wijnands et al. 2006; Degenaar et al. 2012), and most recently Swift/XRT (Degenaar & Wijnands 2009, 2010). A number of LMXB systems remain in this luminosity range persistently or quasi-persistently (e.g., in't Zand et al. 2005; Del Santo et al. 2007; Campana 2009; Heinke et al. 2009; Degenaar & Wijnands 2010; Armas Padilla et al. 2013), so their behaviour is not always transient. Monitoring of X-ray bursts with BeppoSAX's WFC identified a number of thermonuclear X-ray bursts from locations without evidence of persistent emission above $L_X \sim 10^{35}$ ergs/s. These "burst-only" sources (Cocchi et al. 2001; Cornelisse et al. 2002b,a; Campana 2009) are also thought to be producing

bursts during episodes of low-level accretion. X-ray binaries with peak L_X in the range 10^{34} – 10^{36} ergs/s are known as very-faint X-ray binaries (VFXBs). The low time-averaged accretion luminosity of VFXBs is hard to explain in binary evolution models, since it is difficult to reach mass-transfer rates this low via standard LMXB binary evolution within the age of the universe (King & Wijnands 2006; Degenaar & Wijnands 2010; Maccarone & Patruno 2013).

In this paper, we present a detailed study of the 2013 outburst of the VFXB CXOGC J174540.0-290005. This VFXB was first identified as a transient in a *Chandra* observation in 2003 at $L_X = 3.4 \times 10^{34}$ ergs/s, 23" from Sgr A*, while the sum of other deep *Chandra* observations indicated a quiescent (2–8 keV) L_X upper limit of 4×10^{31} ergs/s (Muno et al. 2005). A Swift-XRT monitoring campaign observed a 2-week-long outburst from a nearby transient starting on 20 Oct. 2006 (Kennea et al. 2006b,a), reaching a peak L_X of 2.3×10^{35} ergs/s on 22 Oct. 2006 (Degenaar & Wijnands 2009). A *Chandra* observation on Oct. 29, 2006 identified this transient as CXO J174540.0-290005 (Degenaar & Wijnands 2009). Wang et al. (2006) used the PANIC near-infrared camera to observe CXOGC J174540.0-290005 on 30–31 October 2006, finding no evidence of an infrared counterpart within the 90% confidence area given by (Muno et al. 2005). However, as Degenaar & Wijnands (2009) note, these observations were taken after CXO J174540.0-290005 had dropped below Swift’s detection limit.

The identification of outbursts reaching above 10^{36} ergs/s from VFXBs that have also shown fainter outbursts indicates that low-luminosity outbursts are a behaviour, not necessarily indicating a fundamentally different class of objects (e.g. Degenaar & Wijnands 2010). Furthermore, VFXB outbursts can be produced by a range of objects, including high-mass X-ray binaries (Torii et al. 1998), symbiotic X-ray binaries (Masetti et al. 2007), and cataclysmic variables (Mukai et al. 2008; Stacey et al. 2011). However, high-mass X-ray binaries or M-giants can be ruled out for most X-ray sources in the Galactic Centre (Laycock et al. 2005; Mauerhan et al. 2009; DeWitt et al. 2010), cataclysmic variables cannot reach the peak luminosities attained by most VFXBs, and neither produce X-ray bursts as have now been seen from numerous VFXBs (Cornelisse et al. 2002b), so LMXBs appear to be the primary source type seen. In some cases VFXB peak luminosities may be due only to geometric effects (observing the system edge-on, so that most of the true luminosity is hidden by the accretion disk, e.g. Muno et al. 2005), though this is unlikely to account for the majority of the systems (Wijnands et al. 2006).

Some VFXBs have high-quality X-ray spectra, and in some cases display spectral evolution, during an outburst. Armas Padilla et al. (2013) identify clear soft thermal components in XMM-Newton spectra of two persistent VFXBs at $L_X \sim 3 \times 10^{34}$ ergs/s, and a relatively soft power-law (photon index $\Gamma = 2.5$) for one at $L_X \sim 10^{35}$ ergs/s. Armas Padilla et al. (2011) found a softening of the 0.5–10 keV X-rays for the transient VFXB XTE J1719-291, over the L_x range from 7×10^{35} ergs/s down to 10^{34} ergs/s, from one XMM-Newton and several Swift/XRT and RXTE observations. Swift J1357.2-0933, believed to be a black hole (Corral-Santana et al. 2013), showed spectral softening in

Swift/XRT data as it declined (Armas Padilla et al. 2013), and its XMM-Newton spectrum revealed evidence for a soft component (Armas Padilla et al. 2013). Degenaar et al. (2012) find significant softening in the persistent VFXB XMMU J174554.1-291542 in multiple XMM observations covering $L_X \sim (4\text{--}10) \times 10^{33} (\text{d}/6 \text{ kpc})^2$ ergs/s, although they suggest (from spectral hardness and an infrared counterpart) that this may be a symbiotic star. A softening during the last stages of outburst decay is commonly observed among luminous X-ray binary outbursts, both from black holes (both stellar-mass black holes, Wu & Gu 2008; Plotkin et al. 2013, and also in AGN at similar Eddington fraction, Constantin et al. 2009; Gültekin et al. 2012), and in neutron stars, where emission from the NS surface may be relevant (Jonker et al. 2003; Degenaar et al. 2013; Linares et al. 2014). For instance, Bahramian et al. (2014) observe hardening during the outburst rise of a bright NS transient, and connect the spectral evolution to the changing optical depth of a hot Comptonizing atmosphere (Deufel et al. 2001).

In anticipation of possible interactions between the Sgr A* supermassive black hole and the infalling gas cloud G2 (Gillessen et al. 2012), X-ray monitoring campaigns of the Galactic Center have been undertaken using Swift-XRT, *Chandra*, and NuSTAR, with which we have serendipitously followed a full outburst of CXOGC J174540.0-290005. The outburst was detected by NuSTAR (Dufour et al. 2013), confirmed and tracked by SWIFT/XRT (Degenaar et al. 2013), and confidently associated with CXO J174540.0-290005 using one of several *Chandra* observations (Heinke et al. 2013). We have simultaneous observations with the Karl G. Jansky Very Large Array (VLA), which we use to place a radio upper limit on CXO J174540.0-290005. The frequency of our X-ray observations during the outburst, along with their sensitivity and wide energy range, allows us to study a very faint LMXB outburst in more detail than is usually possible. In §2 below, we describe the data and spectral analysis from these instruments. In §3, we provide an accurate position for the transient, discuss its lightcurve, spectrum, and spectral variations, and compare its behaviour to that in previous outbursts. In §4 we discuss how our results relate to analyses of low-luminosity NS X-ray binary spectra. Unless otherwise specified, all errorbars are at 90% confidence for one parameter of interest.

2 ANALYSIS OF INDIVIDUAL INSTRUMENTS

This section describes the data and analysis for each instrument, culminating with spectral fits summarized in Table 2 for the X-ray data.

2.1 NuSTAR

Since the discovery of the new magnetar SGR 1745-29 near the Galactic Center (Kennea et al. 2013; Mori et al. 2013), *NuSTAR* has performed 13 target-of-opportunity observations between 4/26/2013 and 8/13/2013. *NuSTAR* detected CXO J174540.0-290005 twice, on 5/18/2013 (ObsID 2013008) and 5/27/2013 (ObsID 2013010) with exposure

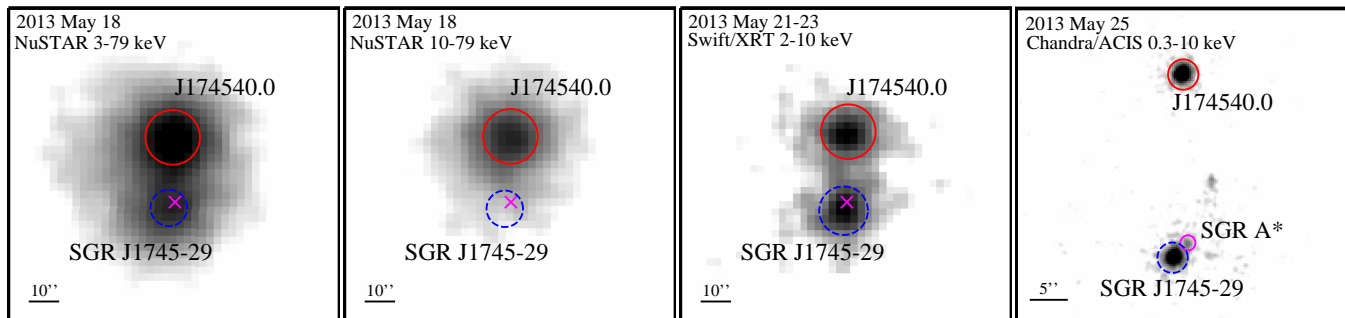


Figure 1. Images of CXO J174540.0-290005 (red circle) from different telescopes (NuSTAR, Swift/XRT, and Chandra/ACIS). The blue dashed circle indicates SGR 1745-29 (clearly visible in all images except NuSTAR 10-79 keV), and the magenta circle or cross indicates the position of Sgr A* (visible only in the Chandra image).

times of 39.0 and 37.4 ksec. In this section, we present *NuSTAR* spectral analysis of CXO J174540.0-290005 using the two detections, and upper limits derived before and after, on 5/11/2013 (ObsID 2013006) and 6/14/2013 (ObsID 2013012).

NuSTAR consists of the two co-aligned X-ray telescopes (FPMA and FPMB) with an energy band of 3-79 keV and spectral resolution of 400 eV (FMHM) at 10 keV (Harrison et al. 2013). Although *NuSTAR* was only able to partially resolve CXO J174540.0-290005 and SGR 1745-29 with its 18'' (FWHM) angular resolution, we carefully removed the contamination from SGR 1745-29 in our spectral analysis. *NuSTAR* data processing and analysis were performed with the *NuSTAR Data Analysis Software (NuSTARDAS)* v.1.2.0.¹ We analyzed *NuSTAR* spectra from FPMA and FPMB separately, but later we jointly fit them using XSPEC.²

Prior to our spectral analysis, we applied an astrometric correction to *NuSTAR* event files by registering SGR 1745-29 to its Chandra position RA = 17h45m40s.169 and DEC = -29deg00'29".84 (J2000) (Rea et al. 2013) in the 3-10 keV band. For the two *NuSTAR* observations, we extracted source photons from a 15'' radius circle around the Chandra position of CXO J174540.0-290005 at RA = 17^h45^m40^s.07 and DEC = -29°00'05".8 (J2000). (See Figure 1.) The source extraction circle was chosen to obtain high signal-to-noise ratio source spectra by minimizing the contamination from SGR 1745-29, located ~ 20'' away from CXO J174540.0-290005, although the contamination was still substantial. We therefore extracted background spectra from pre- and post-outburst *NuSTAR* observations on 5/11/2013 (ObsID: 2013006) and 6/14/2013 (ObsID: 2013012) using the same source extraction region, after verifying that we did not detect CXO J174540.0-290005 in these data. The pre- and post-outburst spectra are identical within statistical uncertainties, so we took the average of the two spectra and used it as a background spectrum. Since the X-ray flux variation of SGR 1745-29 was small during the CXO J174540.0-290005 outburst (Kaspi & et al 2014), the contamination due to SGR 1745-29, as well as diffuse background in the Galactic Center, should be subtracted in our analysis. We binned the *NuSTAR* spectra using *grppha* to attain a min-

imum of 30 counts per bin. After background subtraction, the net *NuSTAR* 3-79 keV count rates are 0.103 ± 0.002 and 0.108 ± 0.002 cts/sec for FPMA and FPMB respectively.

To measure upper limits on CXO J174540.0-290005's flux for ObsIDs 2013006 and 2013012, we performed a similar analysis, taking background spectra from the observations before and after the outburst, respectively. For these observations, the flux normalization was consistent with zero at the 1- σ level.

We performed spectral analysis of the *NuSTAR* detections in 2-79 keV using HEASOFT 6.13 and XSPEC 12.8.1 with CALDB 20130509, and considered an absorbed power-law model to fit the data, using the TBABS absorption model with Wilms et al. (2000) abundances and Verner et al. (1996) cross-sections. Both *NuSTAR* modules (A & B) were considered as a single data group and were jointly fit. We find that the *NuSTAR* spectra are well fit (reduced χ^2 of 1.01 and 0.99 for 2013008 and 2013010, respectively; see Table 2, Figure 2) with absorbed power-law models, with photon indices of 1.73/1.72 in each, though the flux decreased by a factor of two in nine days. These measurements are of particular interest as they are the first *NuSTAR* spectra from an LMXB with an L_X of a few $\times 10^{35}$ ergs/s. The *NuSTAR* spectra do not show obvious evidence (e.g. strong residuals to the power-law fit) of curvature (apart from that attributable to $N_H \sim 2.6 \times 10^{23}$ cm⁻² at the soft end); e.g. Fig. 2. We note that the inferred unabsorbed 2-79 keV flux is 3.1 times the unabsorbed 2-10 keV flux, which agrees with in't Zand et al. (2007)'s estimate that $L_{\text{bol}} \sim 3L_X(2-10 \text{ keV})$.

Fitting the *NuSTAR* spectra with a physically motivated Comptonization model (*TBABS*COMPTT* in XSPEC, Titarchuk 1994) also gives a reasonable fit (reduced χ^2 of 1.01 and 0.99 respectively; see Table 3). The brighter *NuSTAR* spectrum, from ObsID 2013008 on May 18, gives only a lower limit (95% single-sided confidence interval) of 40 keV for the Comptonizing electron temperature, at $L_X(2-10 \text{ keV}) = 3.5 \times 10^{35}$ ergs/s. The fainter *NuSTAR* spectrum, at only 1.8×10^{35} ergs/s, however, shows weak evidence of a spectral turnover, measuring $kT_e = 14_{-3}^{+96}$ keV (90% confidence range) for the Comptonizing electron temperature. Although this fit suggests a relatively low Comptonizing electron temperature, it is not highly constraining—an electron temperature of 100 keV is still allowed.

The *NuSTAR* data do not show strong evidence of lines from CXO J174540.0-290005. We tested a fit including an

¹ <http://heasarc.gsfc.nasa.gov/docs/nustar/analysis/>

² <http://heasarc.gsfc.nasa.gov/docs/xanadu/xspec/>

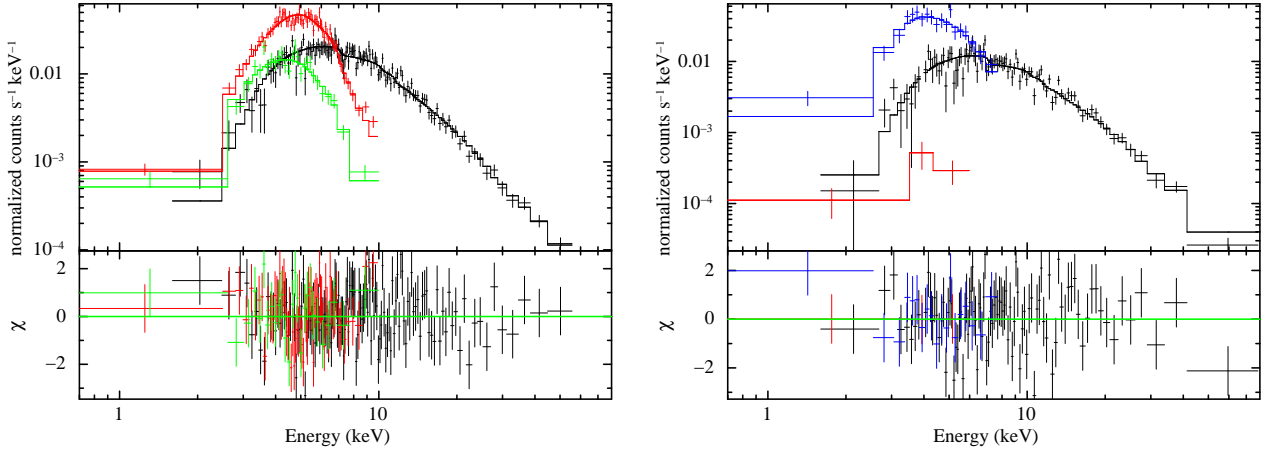


Figure 2. Key spectra of CXO J174540.0-290005 fit with an absorbed powerlaw (see text for details), showing data and model (top) and residuals in units of $\Delta\chi^2$ (bottom). *Left:* NuSTAR ObsID 2013008 (black), Chandra/ACIS zeroth-order spectrum for ObsID 15040 (red), Chandra/ACIS ObsID 14703 (green). *Right:* NuSTAR ObsID 2013010 (black), Swift/XRT spectra from merged ObsIDs 91736040-42 (blue), and Chandra/ACIS ObsID 14946 (red).

iron line with σ fixed to 0.1 keV, and energy allowed between 6 and 7 keV. For ObsID 2013008, we found that the best-fit line energy at 6.8 keV gave an improvement of only 3.4, losing 2 degrees of freedom, in the χ^2 of 472.7 for a power-law fit. An F-test indicates that there is a 20% likelihood of obtaining such an improvement by chance, and therefore that there is not strong evidence for an iron line in this spectrum. ObsID 2013010 gives similar results.

Some models (e.g. Cumming et al. 2001) suggest that high mass transfer rates may screen the magnetic field of accreting NSs in LMXBs, motivating searches for pulsations in low-mass-transfer-rate LMXBs, such as VFXBs. We searched for periodic and quasi-periodic signals in the NUSTAR data (sensitive to signals between the Nyquist frequency and half of the frequency resolution of our *NuSTAR* data; van der Klis 1989). We studied the source power spectra performing Fast Fourier Transforms (FFTs; see Fig. 3) using the *Xronos* analysis software. We did not find any periodic or quasi-periodic signal in any of the *NuSTAR* observations, nor when considering smaller chunks of data (we accounted for the number of bins searched, and the different degrees of freedom of the noise power distribution in the non-detection level; see Vaughan et al. 1994; Israel & Stella 1996).

We computed the 3σ upper limits on the sinusoidal semi-amplitude pulsed fraction (*PF*), computed according to Vaughan et al. (1994) and Israel & Stella (1996). The deepest limits were obtained using observation ObsID 2013008 during the LMXB outburst. The pulsed fraction limit in the 3–79 keV energy band is $<22\%$ for periods below 100 Hz, rising to $\lesssim 30\%$ for 800 Hz (see Fig. 3). The derived pulsed fraction limits do not consider non-detections due to Doppler smearing, which may be significant in an LMXB such as this, but we do not have sufficient signal to perform a full acceleration search. The typical pulse fractional amplitudes for accreting millisecond X-ray pulsars are a few percent, although some reach up to 30% (Patruno & Watts 2012). Thus, our upper limits do not strongly constrain whether CXO J174540.0-290005 is an accreting millisecond pulsar.

2.2 Swift/XRT

The region surrounding Sgr A* was observed almost daily using the Swift X-ray Telescope (Swift/XRT, effective energy range 0.5–10 keV, Burrows et al. 2005) from May to July 2013 as part of the Sgr A* Swift Monitoring Program (Degenaar et al. 2013). This program enabled the detection of the new magnetar SGR J1745-29 (Mori et al. 2013; Kennea et al. 2013), and of CXO J174540.0-290005 in outburst 20" north of Sgr A*. The outburst of CXO J174540.0-290005 was first detected by *Swift* on 15 May, and was visible to Swift for ~ 3 weeks. We analyzed 38 *Swift/XRT* observations in photon counting (PC) mode from 11 May to 13 July 2013, which represents about 38 ks of observation time. Observations were summed into several groups, based on similar count rates, to improve constraints during spectral fitting (see Table 2.4). We also used archival data from 15 to 31 October 2006 when this object was last observed in outburst (Degenaar & Wijnands 2009), for comparison. This represents an additional 15 data sets and about 23 ks of observation time.

The data was reduced and analyzed using HEASOFT 6.13 and FTOOLS³ (Blackburn 1995) following the *Swift/XRT* analysis threads⁴. The FTOOLS routine *xselect* was used to extract a spectrum from a circular source with a 10" radius and background region, near the source, from each group of observations. Due to the close proximity of SGR 1745-29 in outburst, we reduced the extraction radius (down to 6") as the luminosity decayed, to reduce the contaminating counts from SGR 1745-29. We did not correct for pile-up, since the 2013 outburst peak count rate only reached 0.19 count s^{-1} , well below the lower limit of 0.5 count s^{-1} where pile-up becomes significant⁵. Similarly, the 2006 outburst reached a peak count rate of 0.09 count s^{-1} , and did not require pileup corrections. The FTOOLS routine *xrtmkarf* was used to create ancillary response function

³ <http://heasarc.gsfc.nasa.gov/ftools/>

⁴ <http://www.swift.ac.uk/analysis/xrt/>

⁵ <http://www.swift.ac.uk/analysis/xrt/pileup.php>

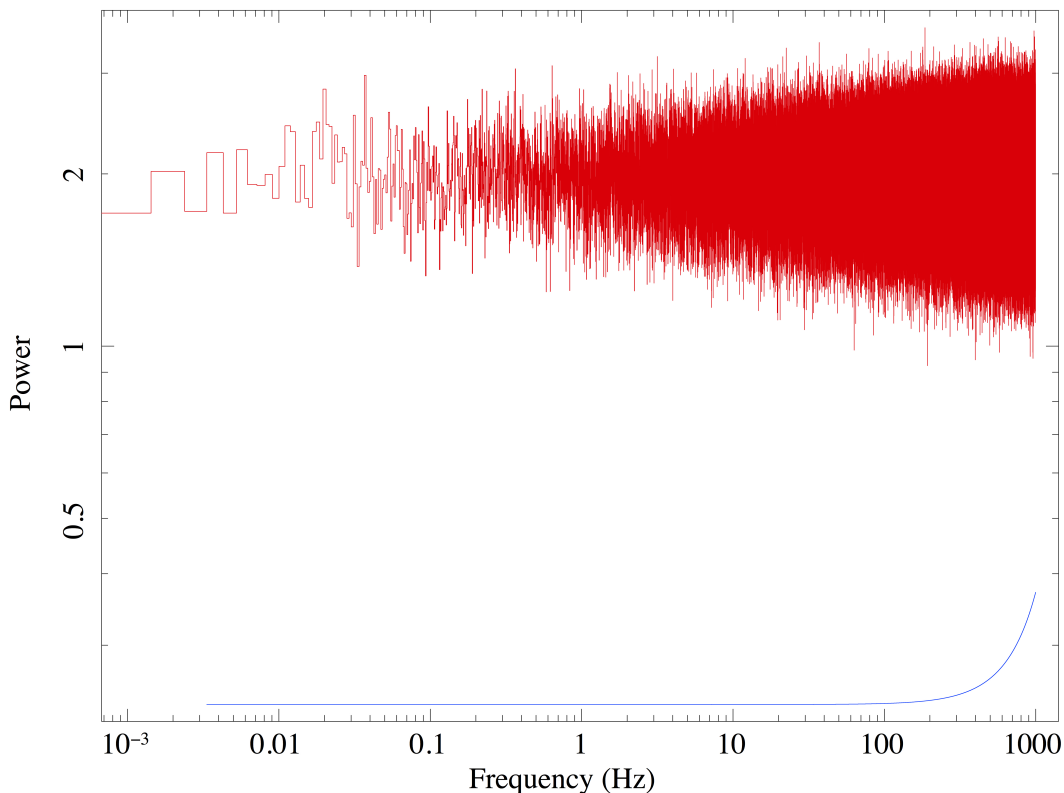


Figure 3. Power spectrum (red) of CXO J174540.0-290005 from *NuSTAR* ObsID 2013008, showing no evidence for pulsations. Blue solid line indicates the pulsed fraction limit as a function of frequency, in units of 100%(0.1=10%), with the pulsed fraction upper limit gradually rising above 100 Hz.

(ARF) files for each group. Spectral analysis was performed using XSPEC 12.8.0 (Arnaud 1996).

The count rates, or count rate limits, for each Swift/XRT observation (see Table 1) were derived by counting the photons within a specified radius, 14" for the high-flux measurements, or 6" for the lowest-flux measurements. We measured backgrounds from a region at roughly the same distance from SGR 1745-29, except for the lowest-flux measurements where an annulus around SGR 1745-29 at the same distance as the (excluded) source extraction region was used. From the Poisson upper bounds at 95% confidence (Gehrels 1986), we calculate upper bounds on the count rates within a 10" radius of the object's position, using an enclosed energy of 50% within this region (Moretti et al. 2005). We used *PIMMS*⁶ with the corrected count rate and the model parameters found during spectral fitting (see §3.2 and Table 2) to calculate an unabsorbed flux in the 2-10 keV energy range. The luminosities, and luminosity upper limits, assumed a distance of 8.0 kpc to CXO J174540.0-290005.

The Swift/XRT lightcurve, due to its regular, frequent sampling, is essential for understanding the overall shape

of the 2013 outburst of CXO J174540.0-290005 (Figure 4). The short Swift/XRT observations do not provide precise measurements of the photon index as provided by the other two X-ray instruments, though they are generally consistent. We combined Swift/XRT spectra from adjacent days (see MJD column of Table 2) to obtain the best possible constraints. There are hints of variations in the hardness (quantified by the fitted photon index; Table 2, Figure 1 right) in the Swift/XRT data, although these are not confirmed by the longer and more sensitive *Chandra* and *NuSTAR* observations, often taken at, or nearly at, the same time. The faintest Swift/XRT measurements (data after MJD 56441) are too heavily contaminated by SGR 1745-29 to provide useful spectra. See §3.4 below for comparison to previous outbursts of this source.

2.3 Chandra/ACIS

The *Chandra/ACIS* combination gives high resolution imaging and spectroscopy, with 0.5" spatial resolution and typically < 0.3 keV energy resolution, over the energy range 0.5-10.0 keV (Weisskopf et al. 2002). The High-Energy Transmission Grating (HETG) can be placed into the optical path, diffracting ~50% of the photons from a point source

⁶ <http://asc.harvard.edu/toolkit/pimms.jsp>

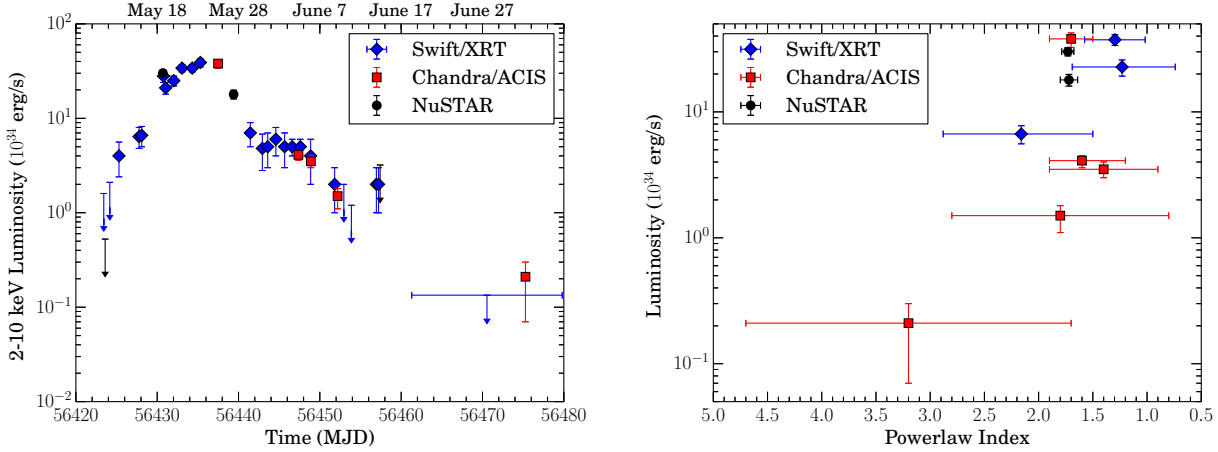


Figure 4. *Left:* The light curve of the outburst using *Swift/XRT* (blue diamond), *Chandra/ACIS* (red squares) & *NuSTAR* (black circles) observations. *Swift/XRT* data points that cover more than one day are merged observations. Note that only statistical uncertainties are included in the X-ray error bars. *Right:* The spectral evolution of the outburst shown with *Chandra/ACIS* (red), *NuSTAR* (black), and *Swift/XRT* (blue).

into spectra dispersed by energy on the detector, with very high energy resolution⁷. The High Energy Grating (HEG) and Medium Energy Grating (MEG) are optimized for different energy ranges, while the undiffracted photons produce a zeroth-order image on the detector.

We observed the region surrounding Sgr A* regularly from 25 May 2013 to 27 July 2013 for a combined *Chandra* exposure of 132 ks over 6 observations (see Table 2.4). Three observations (Obs IDs: 15040, 15651, 15654) were performed using *Chandra/ACIS* with a 1/2 sub-array (to reduce the readout time for the CCD) and HETG, due to the brightness of SGR 1745-29 and CXO J174540.0-290005. This enabled a dispersed grating spectrum of CXO J174540.0-290005 to be extracted for the initial observation on 25 May. However, CXO J174540.0-290005 had dimmed significantly in the subsequent observations, and the dispersed grating spectra were not of sufficient S/N to be usable. The other three observations (Obs ID: 14703; Obs ID: 14946; Obs ID: 15041) were taken with *Chandra/ACIS* in a 1/8 sub-array. Archival *Chandra* data was also reanalyzed, from the 2003 (Muno et al. 2005) and 2006 (Degenaar & Wijnands 2009) outbursts (see Table 1), for an additional 30 ks of observation time.

All *Chandra* data were reduced and analyzed using CIAO 4.5 (Fruscione et al. 2006) following the CIAO science threads⁸. Each data set was reprocessed using the CIAO routine *chandra_repro*. Undispersed spectra from each observation were extracted using the CIAO tool *specextract*. Source extraction regions were optimized for maximal S/N ratio, and background was extracted from a surrounding annulus when the source was faint, or a nearby region when bright.

In ObsID 15041 (45 ks long), CXO J174540.0-290005 was not detected. We estimate a count excess of $7.7_{-8.0}^{+10.2}$ counts over background (2-5 keV) at this location, which we conservatively interpret as an upper limit of 18 counts (at

90% confidence). We calculate an intrinsic L_X limit from our countrate limit using either a $\Gamma=1.7$ power-law, or an NSATMOS hydrogen-atmosphere neutron star model (assuming a $1.4 M_\odot$ and 10 km NS) (Heinke et al. 2006), finding in either case $L_X(2-10 \text{ keV}) < 4 \times 10^{32}$ ergs/s. This gives a temperature of $< 1.9 \times 10^6$ K and indicates that CXO J174540.0-290005 has returned to quiescence.

Dispersed grating spectra were extracted with the CIAO routine *tgextract* as per the HETG/ACIS science thread⁹, taking care not to include the dispersed spectra from SGR 1745-29 in the spectra or backgrounds for CXO J174540.0-290005. The first order grating spectra (HEG and MEG) were combined using the CIAO routine *add_grating_orders*. The +1 and -1 order response matrix files (RMFs) were found to be indistinguishable, so we used the -1 order RMFs for both. We analyzed the first order grating spectra (a combined first-order HEG spectrum, and combined first-order MEG spectrum) from the *Chandra/ACIS* ObsID 15040. Unfortunately, the total counts were only 860 and 745 in the combined MEG first-order and HEG first-order spectra respectively, with less than 40 counts in each higher-order spectrum (hence, we ignore the higher-order spectra). Furthermore, the HEG spectrum of CXO J174540.0-290005 suffers from a dispersion angle that places it quite close to that of SGR 1745-29, and overlapping with the complex around Sgr A*, making background subtraction difficult.

We first bin the grating spectra by a factor of 10 in wavelength, undersampling the spectral resolution by a factor of two, to look for any signs of emission or absorption lines. We use an absorbed powerlaw model (as fit to the undispersed spectra) for our continuum. Although there are weak suggestions of emission lines at 4.5, 4.9, and 6.4 keV in the combined MEG spectrum (none significant), these energies show only suggestions of absorption in the combined HEG spectrum. We therefore provide only upper limits on the flux from narrow ($\sigma=0.1$ keV) emission lines at these locations,

⁷ <http://cxc.harvard.edu/proposer/POG/html/chap8.html>

⁸ <http://cxc.harvard.edu/ciao/threads>

⁹ http://cxc.harvard.edu/ciao/threads/spectra_multi_acis

using the MEG spectrum; at 6.4 keV, $F_X < 1.4 \times 10^{-12}$ erg $\text{cm}^{-2} \text{s}^{-1}$ (Equivalent width of < 0.07 keV); at 4.5 keV, $F_X < 1.8 \times 10^{-12}$ erg $\text{cm}^{-2} \text{s}^{-1}$ (Equivalent width of < 0.09 keV), or at 4.9 keV, $F_X < 1.9 \times 10^{-12}$ erg $\text{cm}^{-2} \text{s}^{-1}$ (Equivalent width of < 0.06 keV). We also group the data to require 20 counts/bin, and perform independent fits to the continuum of the MEG and HEG data. We find values for the photon index (1.5 ± 0.9 or 1.9 ± 1.0 , respectively) and flux ($5.2_{-0.8}^{+1.2} \times 10^{-11}$ or $4.4_{-0.9}^{+1.2} \times 10^{-11}$ erg $\text{cm}^{-2} \text{s}^{-1}$) from the MEG and HEG data that are consistent with (but with larger errors than) the fit to the simultaneous zeroth-order undispersed spectrum (Table 2).

All of the *Chandra* spectra (undispersed, and dispersed) are consistent with an absorbed power-law of photon index consistent with 1.7 (see Table 2). Pileup effects were considered when modeling the bright undispersed spectra, as the peak count rate reaches ≈ 0.2 ct/s, even though the data were taken using subarrays (see §3.2). The *Chandra* undispersed spectra provide the highest-quality data at low energies, which we use below to obtain the best estimate of N_H (§3.2). The *Chandra* data also provide the highest-precision position for CXO J174540.0-290005 (§3.1).

2.4 VLA

We carried out radio continuum VLA imaging of the Sgr A* region on May 25, 2013, simultaneous with *Chandra* ObsID 15040. A detailed account of these observations will be given elsewhere. Briefly, radio data were taken with the VLA in its BnC configuration at 0.7 cm. We used the new correlator setup employing 2 GHz bandwidth around 43 GHz. The initial calibration was done with OBIT (Cotton 2008) employing the phase calibrators J1744-3116, J1733-1304 and the absolute calibrator 3C286. Imaging was performed in AIPS with a resolution of $1.3'' \times 1.1''$ (PA $\sim -89^\circ$). Unfortunately CXO J174540.0-290005 is projected against the edge of the northern arm of the minispiral (Ekers et al. 1983), producing a very high radio continuum background, and CXO J174540.0-290005 was not detected in this observation. The rms noise of the image per beam, after phase and amplitude self-calibration, is ~ 2 mJy.

Different correlations between radio and X-ray luminosities have been observed for black holes (Corbel et al. 2003; Gallo et al. 2006, 2012) vs. for neutron stars (Migliari & Fender 2006). Thus, measuring the radio flux of an unknown X-ray luminous object can help to determine its nature. However, the radio upper limit we derive here is rather shallow. For a distance of 8 kpc, we calculate a radio luminosity $1-\sigma$ upper limit (up to 8.5 GHz, assuming a flat spectrum) of 3.3×10^{30} , compared with a simultaneous *Chandra* X-ray measurement of $L_X(2-10 \text{ keV}) = 4 \times 10^{35}$ ergs/s. This upper limit is well above the radio detections of similarly-luminous neutron star X-ray binaries (Migliari & Fender 2006), and also above the radio detections of all similarly luminous black hole X-ray binaries (e.g. Gallo et al. 2012). Thus, due to the high continuum background at this location and the relative faintness of this transient, we cannot draw conclusions from the radio non-detection, and cannot distinguish whether this VFXB contains a neutron star or a black hole.

3 KEY RESULTS

3.1 Position

The position of the new transient was derived using *Chandra/ACIS* ObsID 15040, in which both SGR 1745-29 and the transient were clearly detected using the *wavdetect* program (Figure 1; see also Heinke et al. 2013). The position of SGR 1745-29 was calculated by Shannon & Johnston (2013), using an ATCA radio interferometric observation, to be RA= 17:45:40.16 \pm 0.022" and Dec= -29:00:29.82 \pm 0.09". We thus shifted our *Chandra* positions to find the astrometrically corrected position of the new transient, RA= 17:45:40.07 \pm 0.1" and Dec= -20:00:05.8 \pm 0.1". This result agrees with the published position of CXO J174540.0-290005, RA= 17:45:40.06 \pm 0.6" and Dec= -29:00:05.5 \pm 0.6" (Muno et al. 2005; Degenaar & Wijmands 2009), confirming the identification. We adopt this updated, boresited position for CXO J174540.0-290005 for our entire analysis. The close proximity of CXO J174540.0-290005 to Sgr A*, 23" or 0.9 parsecs in projection, given the concentration of X-ray sources and transients close to Sgr A* (Muno et al. 2003, 2005), strongly indicates that the distance to CXO J174540.0-290005 is essentially identical to that of Sgr A*, for which we adopt 8 kpc Reid (1993). The high absorption, consistent with other sources near Sgr A* Muno et al. (2003), agrees with the adopted distance.

3.2 Column Density

Since the individual spectra were typically not sufficient to effectively constrain the column density, we first conducted joint spectral fits designed to measure N_H . Two joint fits were performed (Table 2), one for the 6 groups of *Swift/XRT* data, and the other for the *Chandra/ACIS* data, due to the differing fractions of the dust scattering halo that would be encompassed in the spectral extractions from the two instruments. Dust scatters a fraction of the X-rays out of the line of sight, typically at small angles (e.g. Predehl & Schmitt 1995). For the expected distribution of dust towards Galactic Center sources (much of the dust within 100 pc), $\sim 50\%$ of the scattered 2 keV X-rays should be found within a 1" scattering halo of Sgr A* (Tan & Draine 2004), whereas virtually all the scattered halo should lie within the *Swift/XRT* extraction region. We used the photoionization cross sections given by Verner et al. (1996), and abundances from Wilms et al. (2000), in our photoelectric absorption model.

We used an absorbed powerlaw to model the data, taking into account scattering with the SCATTER model (Predehl et al. 2003), (PILEUP \times TBABS \times PEGPWRLW \times SCATTER), to model the *Chandra/ACIS* spectra. The dust extinction parameter A_V was set to $n_H/0.177$ and α in the pileup model was frozen to 0.5 as per Davis (2001). Freeing the pileup parameter α did not substantially alter our results.

Since our extraction region was several times the expected scattering halo size for the *Swift/XRT* and *NuSTAR* spectra, and pileup was not a concern, we simplified our model for these data to TBABS \times PEGPWRLW. The power-law photon indices and flux normalizations for each observation were left untied during fitting. The column density value from our joint *Chandra/ACIS* fit, $N_H = 15.1_{-1.4}^{+1.6} \times 10^{22} \text{ cm}^{-2}$,

Table 1. X-ray observations of CXO J174540.0-290005 during 2013.

Observation ID	Date	Exposure Time	Luminosity ($\times 10^{34}$ erg s $^{-1}$)	Notes*
91736031	2013-05-11	957 s	< 1.6	
N-2013006	2013-05-11	32.6 ks	<0.5	
91736032	2013-05-12	926 s	< 2.1	
91736033	2013-05-13	958 s	4.0 ± 1.6	
91736035	2013-05-15	941 s	6.4 ± 1.6	1
91736036	2013-05-16	987 s	6.6 ± 1.6	1
N-2013008	2013-05-18	38.8 ks	35 ± 2	2
91736037	2013-05-18	956 s	28 ± 4	1
91736038	2013-05-19	952 s	21 ± 3	1
91736039	2013-05-20	1006 s	25 ± 3	
91736040	2013-05-21	978 s	34 ± 3	
91736041	2013-05-22	1005 s	34 ± 3	
91736042	2013-05-23	958 s	39 ± 4	
C-15040	2013-05-25	24.4 ks	38^{+4}_{-3}	3
N-2013010	2013-05-27	37.3 ks	18 ± 2	
91712006	2013-05-29	956 s	7 ± 2	
91736044	2013-05-30	972 s	4.8 ± 2	
91736045	2013-05-31	991 s	5 ± 2	
91736046	2013-06-01	872 s	6 ± 2	
91736047	2013-06-02	1036 s	5 ± 2	
91736048	2013-06-03	1044 s	5 ± 1	
91736049	2013-06-04	1007 s	5 ± 1	
C-14703	2013-06-04	18.6 ks	$4.1^{+0.5}_{-0.4}$	
91712007	2013-06-05	980 s	4 ± 2	
C-15651	2013-06-05	14.1 ks	3.5 ± 0.5	
91736052	2013-06-08	1119 s	2 ± 1	
91736053	2013-06-09	947 s	< 2.0	
C-15654	2013-06-09	9.3 ks	$1.5^{+0.4}_{-0.3}$	
91736054	2013-06-10	957 s	< 1.2	
91736056	2013-06-13	1250 s	2 ± 1	
91736057	2013-06-14	941 s	2 ± 1	
N-2013012	2013-06-14	26.8 ks	<3.2	
91736061	2013-06-18	992 s	<2.0	
91712009	2013-06-19	1067 s	<2.5	
91736062	2013-06-20	1020 s	<3.2	
91736063	2013-06-21	1079 s	<4.8	
91736064	2013-06-24	1050 s	<3.2	
91736065	2013-06-25	1085 s	<3.7	
91712010	2013-06-26	756 s	<2.6	
91736066	2013-06-28	1001 s	<2.6	
91736068	2013-06-29	1146 s	<3.4	
91736069	2013-06-30	937 s	<4.0	
91736070	2013-07-01	955 s	<2.9	
91736071	2013-07-02	955 s	<4.2	
C-14946	2013-07-02	20.1 ks	$0.38^{+0.23}_{-0.15}$	
91712011	2013-07-03	1061 s	<4.0	
91736073	2013-07-05	1019 s	<4.2	
91736074	2013-07-06	970 s	<4.5	
C-15041	2013-07-27	45.4 ks	<0.04	

List of observations used in our analysis, with 2-10 keV L_X estimates. ObsIDs have a C- for Chandra, N- for *NuSTAR* (omitting the 8000 at the beginning of each *NuSTAR* ObsID), or refer to Swift/XRT observations. * References to previous analyses of these observations: - (1) Degenaar et al. (2013); (2) Dufour et al. (2013); (3) Heinke et al. (2013).

was well-constrained. The column density value for the *Swift/XRT* fit was $N_H = 12.6^{+3.5}_{-3.0} \times 10^{22} \text{ cm}^{-2}$, consistent with the *Chandra/ACIS* value but with larger errors. The neutral N_H column in low-mass X-ray binaries of low to moderate inclination seems empirically to remain constant during outbursts (Miller et al. 2009), except for the highest L_X

outbursts (Oosterbroek et al. 1997; Życki et al. 1999). We therefore used the *Chandra/ACIS* measurement as our N_H value in analyses of individual Chandra and Swift spectra. The *NuSTAR* spectral fits require a larger value of $N_H = 2.6 \times 10^{23} \text{ cm}^{-2}$ for power-law fits. We note that although the formal uncertainties are small ($3 \times 10^{22} \text{ cm}^{-2}$

Table 2. Fits to 2003, 2006, & 2013 X-ray spectra of CXO J174540.0-290005

Observation ID	MJD	N_H ($\times 10^{22} \text{ cm}^{-2}$)	Photon Index	Flux ($\times 10^{-12} \text{ erg cm}^{-2} \text{ s}^{-1}$)	L_X (2-10 keV) (erg s^{-1})	D.O.F.	Red. χ^2
2003							
C-03549	52809.8	15.1 (fixed)	1.6 \pm 0.2	6.6 \pm 0.3	5.1 \pm 0.2 $\times 10^{34}$	26	0.93
2006							
3564978-84	54023.0-54029.0	15.1 (fixed)	1.9 \pm 0.6	4.1 \pm 0.7	3.3 \pm 0.5 $\times 10^{34}$	32	0.88
3564985	54030.1	t	1.5 $^{+0.6}_{-0.7}$	19.4 $^{+4.0}_{-3.6}$	1.5 \pm 0.3 $\times 10^{35}$	t	t
3564986-87	54031.1-54032.0	t	1.7 \pm 0.5	13.4 \pm 2.0	1.0 \pm 0.2 $\times 10^{35}$	t	t
3564988-92	54032.9-54039.5	t	2.0 \pm 0.4	5.6 \pm 0.6	4.3 \pm 0.5 $\times 10^{34}$	t	t
06646	54037.1	t	1.7 \pm 0.6	2.4 \pm 0.4	1.8 \pm 0.3 $\times 10^{34}$	t	t
2013							
C-15040	56437.5	15.1 $^{+1.6}_{-1.4}$	1.7 \pm 0.2	49.7 $^{+5.5}_{-4.4}$	3.8 $^{+0.4}_{-0.3}$ $\times 10^{35}$	178	0.75
C-14703	56447.4	t	1.6 $^{+0.4}_{-0.3}$	5.4 $^{+0.6}_{-0.5}$	4.1 $^{+0.5}_{-0.4}$ $\times 10^{34}$	t	t
C-15651	56448.9	t	1.4 \pm 0.5	4.6 \pm 0.6	3.5 \pm 0.5 $\times 10^{34}$	t	t
C-15654	56452.2	t	1.8 \pm 1.0	2.0 $^{+0.5}_{-0.4}$	1.5 $^{+0.4}_{-0.3}$ $\times 10^{34}$	t	t
C-14946	56475.3	t	3.2 $^{+1.5}_{-1.5}$	0.29 $^{+0.18}_{-0.13}$	2.1 $^{+1.4}_{-0.9}$ $\times 10^{33}$	t	t
91736031-36	56423.4-56428.1	15.1 (fixed)	2.2 $^{+0.8}_{-0.9}$	6.1 \pm 1.3	4.6 \pm 0.8 $\times 10^{34}$	43	0.64
91736037-39	56430.8-56432.0	t	1.2 $^{+0.4}_{-0.5}$	31 \pm 4	2.4 \pm 0.3 $\times 10^{35}$	t	t
91736040-42	56433.1-56435.3	t	1.2 \pm 0.3	50 \pm 5	3.8 \pm 0.4 $\times 10^{35}$	t	t
91736044-47 & 91712006	56441.5-56445.7	t	2.0 \pm 0.7	8 \pm 1	6 \pm 1 $\times 10^{34}$	t	t
91736048-57 & 91712007	56446.6-56457.2	t	2.1 \pm 0.7	4.6 $^{+0.8}_{-0.7}$	3.4 $^{+0.7}_{-0.6}$ $\times 10^{34}$	t	t
N-2013008	56430.7	25 \pm 3	1.73 \pm 0.08	39 \pm 3	3.5 \pm 0.2 $\times 10^{35}$	467	1.01
N-2013010	56439.4	27 \pm 5	1.72 \pm 0.08	23 $^{+3}_{-2}$	1.8 \pm 0.2 $\times 10^{35}$	337	0.99

Joint and individual fits of the *Swift*/*XRT*, *Chandra*/*ACIS* (indicated with C-) and *NuSTAR* (indicated with N-) data sets. Luminosities are calculated using a distance of 8.0 kpc. The luminosity and flux are calculated over the 2-10 keV range.

Table 3. Comptonization Model Fits to NuSTAR Spectra of CXO J174540.0-290005

Obs. ID	N_H (10^{22} cm^{-2})	T_0 (keV)	kT (keV)	τ	$\chi^2/\text{d.o.f}$
2013008	16 $^{+6}_{-5}$	1.1 $^{+0.2}_{-0.3}$	>40	0.05 $^{+1.28}_{-0.01}$	469.72/465
2013010	21 $^{+8}_{-9}$	0.9 $^{+0.3}_{-0.9}$	14 $^{+96}_{-3}$	3.04 $^{+0.7}_{-2.96}$	331.84/335

Details of *TBABS*COMPITT* spectral modeling of the two NuSTAR observations of CXO J174540.0-290005.

for the first ObsID), there are complexities in the NuSTAR background subtraction at low energies (where SGR 1745-29 dominates the flux). The N_H values obtained from these fits are consistent with a location at the Galactic Center, as expected given the close proximity to Sgr A*.

3.3 Lightcurve and Spectral Evolution

Figure 4 (left) shows the lightcurve of CXO J174540.0-290005 over the entire outburst. It rose from L_X (2-10 keV) $< 5 \times 10^{33}$ ergs/s on May 11 up to 4.0×10^{34} ergs/s on May 13, and then to a peak of 3.8×10^{35} ergs/s on May 18. The lightcurve shows evidence for a dip of almost a factor of two for a few days, then recovers and reaches a briefly higher peak on May 25, at 5.0×10^{35} ergs/s, before rapidly declining by a factor of seven over four days. The lightcurve then decays more slowly, by a factor of two over ten days, before falling below Swift/*XRT*'s detection limit.

A final *Chandra* observation another 24 days later finds CXO J174540.0-290005 another factor of ~ 7 fainter, at $2.1^{+1.4}_{-0.9} \times 10^{33}$ erg s $^{-1}$, and possibly with a softer spectrum (the best-fit photon index was $3.2^{+1.5}_{-1.5}$, not significantly different than at higher L_X). The Swift/*XRT* upper flux limit, averaged over the last 20 days, is slightly lower than the flux from the last *Chandra* observation (near the end of those 20 days), suggesting that the flux measured in the final *Chandra* observation was not persistent throughout that time period. It is clear that the outburst as a whole did not last longer than 26 days above 4×10^{34} ergs/s, with a total 2-10 keV (unabsorbed) fluence of $\sim 4.7 \times 10^{-5}$ ergs cm $^{-2}$, or for an 8.0 kpc distance (considering its proximity to Sgr A*), a total 2-10 keV emitted energy of $\sim 3.6 \times 10^{41}$ ergs.

An absorbed powerlaw model adequately fits all the datasets (see Table 2, and Figure 2). We plot the variation in the fitted power-law photon index (chosen as a more instrument-independent quantity than hardness ratios) in Figure 4 (right). The data are consistent with a fixed photon

index of $\Gamma = 1.7$ for all observations. There is a slight suggestion of spectral evolution in the Swift/XRT data alone (Figure 4, Table 2), indicating softening during the decline from 2×10^{35} ergs/s and 6×10^{34} ergs/s. However, this is not supported by the (higher-statistics) Chandra data, which show no evidence of spectral changes between observations at the peak L_X (4×10^{35} ergs/s) down to 1.5×10^{34} ergs/s. The average fitted photon indices from the Chandra, Swift/XRT, and NuSTAR data agree quite well.

3.4 Comparison to Previous Outbursts

The Galactic Center has been monitored regularly using the Swift/XRT telescope since 2006, sometimes on a daily basis, in other years typically every third day (Degenaar & Wijnands 2009; Degenaar et al. 2013). Two outbursts of CXO J174540.0-290005 have now been monitored by Swift/XRT (Degenaar & Wijnands 2009), while a glimpse of a previous outburst was provided serendipitously by *Chandra* (Muno et al. 2005). The 2006 outburst lasted for roughly two weeks with a peak 2-10 keV L_X of 2×10^{35} ergs/s (Degenaar & Wijnands 2009), thus giving a smaller fluence of 1.3×10^{-5} , vs. our measured fluence of 4.7×10^{-5} ergs cm^{-2} . The single 2003 *Chandra* observation found CXO J174540.0-290005 at 3.4×10^{34} erg s^{-1} (2-8 keV) (Muno et al. 2005). If this outburst resembled the two better-studied outbursts of this source, the 2003 observation likely occurred during the outburst tail. We have analyzed the spectra of the previous Chandra and Swift/XRT observations, and find that the spectral parameters (photon index specifically) are consistent with those of our observations (Table 2).

We can re-assess the duty cycle and average mass transfer rate of CXO J174540.0-290005 using the full Swift/XRT campaigns. The total Swift/XRT 2006-2013 campaigns covered roughly 270 weeks. Since the two outbursts observed by Swift/XRT each lasted over 2 weeks, we believe that a similar outburst would have been caught by these observations, which occurred every 1-4 days (excepting periods of ~ 2 months each year when Sgr A* is too close to the Sun for observations). Thus, we estimate a duty cycle of $(2+3)/270 \sim 2\%$, consistent with the 1-6% range estimated by Degenaar & Wijnands (2009). Similarly, the average mass transfer rate, assuming a bolometric luminosity 3 times the 2-10 keV L_X (in't Zand et al. 2007), and a $1.4 M_\odot$, 10 km NS, comes to $\sim 7 \times 10^{-14} M_\odot/\text{year}$, somewhat smaller than the range inferred by Degenaar & Wijnands (2009).

4 DISCUSSION

4.1 Spectra of CXO J174540.0-290005

Few LMXBs with L_X (0.5-10 keV) between 10^{34} and 3×10^{35} ergs/s have high-quality spectra above 10-20 keV, such as our *NuSTAR* spectra provide. Such spectra may enable us to probe how the ‘‘hard’’ accretion state in these systems, which can typically be fit by power-law models without a cutoff up to nearly 100 keV, transitions to the quiescent state. Chakrabarty et al. (2014) have recently shown that the nonthermal component in Cen X-4 shows significant

curvature in quiescence, being well-fit by a bremsstrahlung spectrum of $kT=18 \pm 1$ keV. Possibly the highest-quality data on the hard X-rays during the transition to quiescence are the RXTE (PCA and HEXTE) spectra of SAX J1808.4-3658 (SAX J1808) in its 1998 and 2002 outbursts, since SAX J1808 is not crowded and is relatively nearby (3.5 kpc). Gilfanov et al. (1998) and Gierliński et al. (2002) presented 1998 RXTE spectra of SAX J1808, evolving from $L_X = 3 \times 10^{36}$ ergs/s down to 3×10^{35} ergs/s between 3 and 100 keV, and then dropping down to 3×10^{34} ergs/s (only to 20 keV, Gilfanov et al. 1998), while Ibragimov & Poutanen (2009) presented 2002 RXTE spectra declining from 3×10^{36} down to 3×10^{35} ergs/s between 3-100 keV. These authors all find that SAX J1808’s spectrum remained essentially constant as it declined by over an order of magnitude down to $L_X \sim 3 \times 10^{35}$ ergs/s, though they were unable to clearly detect it above 20 keV below this luminosity. Gierliński et al. (2002) use a Comptonization model for their fits, and find $kT_e = 90_{-30}^{+240}$ keV for a time-averaged spectrum, although they are unable to measure how kT_e may vary across their L_X range. Similarly, Ibragimov & Poutanen (2009) find that a Comptonization model for the higher- L_X spectra requires $kT_e \sim 40$ -45 keV, while it is unconstrained for $L_X = 3 \times 10^{35}$ ergs/s. The LMXB with the faintest peak luminosity to have spectral information above 10 keV is perhaps IGR J17285-2922, a VFXB discovered towards the Galactic bulge with INTEGRAL (Walter et al. 2004). Its two known outbursts have reached (assuming an 8 kpc distance) L_X (2-10 keV) $\sim 5 \times 10^{35}$ ergs/s (in 2003, Barlow et al. 2005), and L_X (2-10 keV) $\sim 4 \times 10^{35}$ ergs/s (in 2010, Sidoli et al. 2011). Both outbursts were observed by INTEGRAL (the second also by XMM), and showed hard time-averaged spectra (Γ of 2.1 ± 0.2 and 1.60 ± 0.01 respectively) extending out beyond 100 keV, without evidence of a spectral turnover (though these INTEGRAL/ISGRI spectra are not high S/N, due to the source faintness).

Thus, our lower-luminosity *NuSTAR* spectrum (ObsID 2013010, see §2.1, Figure 2) is the lowest-luminosity spectral measurement of an LMXB transient in outburst (that we are aware of) above 20 keV. We do not see clear evidence for a spectral turnover below 80 keV, nor do we see differences with higher- L_X spectra. This observation clearly shows that *NuSTAR* can provide excellent hard X-ray spectra of NS X-ray binary transients at even fainter luminosities, if they are closer to Earth (e.g. SAX J1808), allowing us to see how the hard spectra evolve at lower luminosities.

ACKNOWLEDGMENTS

We are very grateful for the hard work by the staff and directors of the observatories, and in particular, to Scott Wolk, Patrick Slane, and Dillon Foight at the CXC, for enabling our monitoring campaigns of the Galactic Center. COH is supported by an NSERC Discovery Grant and an Alberta Ingenuity New Faculty Award. DH is supported by *Chandra* X-ray Observatory (CXO) Award Numbers GO3-14121X, GO3-14099X, and GO3-14060X, operated by the Smithsonian Astrophysical Observatory for and on behalf of NASA under contract NAS8-03060, and also by NASA *Swift* grant NNX14AC30G. NR is supported by a Ramon y Cajal Fellowship, NWO Vidi award, and grants AYA 2012-39303,

SGR2009-811, and iLINK 2011-0303. ND is supported by NASA through Hubble Postdoctoral Fellowship grant number HST-HF-51287.01-A from STScI. This research made use of data obtained from the *Chandra* Data Archive and software provided by the *Chandra* X-ray Center in the application packages CIAO, ChIPS, and Sherpa. The National Radio Astronomy Observatory is operated by Associated Universities Inc., under cooperative agreement with the National Science Foundation. The *Swift*/*XRT* Data Analysis Software (XRTDAS) is developed under the responsibility of the ASI Science Data Center (ASDC), Italy. We acknowledge extensive use of the ADS and arXiv.

REFERENCES

- Armas Padilla M., Degenaar N., Patruno A., Russell D. M., Linares M., Maccarone T. J., Homan J., Wijnands R., 2011, *MNRAS*, 417, 659
- Armas Padilla M., Degenaar N., Russell D. M., Wijnands R., 2013, *MNRAS*, 428, 3083
- Armas Padilla M., Degenaar N., Wijnands R., 2013, *MNRAS*, 434, 1586
- Armas Padilla M., Wijnands R., Altamirano D., Mendez M., Miller J. M., Degenaar N., 2013, arXiv:1308.4326
- Arnaud K. A., 1996, in ASP Conf. Ser. 101: Astronomical Data Analysis Software and Systems V XSPEC: The First Ten Years. p. 17
- Bahramian A., et al. 2014, *ApJ*, 780, 127
- Barlow E. J., et al. 2005, *A&A*, 437, L27
- Blackburn J. K., 1995, in Shaw R. A., Payne H. E., Hayes J. J. E., eds, *Astronomical Data Analysis Software and Systems IV* Vol. 77 of *Astronomical Society of the Pacific Conference Series*, FTOOLS: A FITS Data Processing and Analysis Software Package. p. 367
- Burrows D. N., Hill J. E., Nousek J. A., et al. 2005, *Space Sci. Rev.*, 120, 165
- Campana S., 2009, *ApJ*, 699, 1144
- Chakrabarty D., Tomsick J. A., Grefenstette B. W., et al., 2014, arXiv:1403.6751
- Cocchi M., Bazzano A., Natalucci L., Ubertini P., Heise J., Kuulkers E., Cornelisse R., in't Zand J. J. M., 2001, *A&A*, 378, L37
- Constantin A., Green P., Aldcroft T., Kim D. W., et al. 2009, *ApJ*, 705, 1336
- Corbel S., Nowak M. A., Fender R. P., Tzioumis A. K., Markoff S., 2003, *A&A*, 400, 1007
- Coriat M., Fender R. P., Dubus G., 2012, *MNRAS*, 424, 1991
- Cornelisse R., Verbunt F., in't Zand J. J. M., Kuulkers E., Heise J., 2002, *A&A*, 392, 931
- Cornelisse R., Verbunt F., in't Zand J. J. M., Kuulkers E., Heise J., Remillard R. A., Cocchi M., Natalucci L., Bazzano A., Ubertini P., 2002, *A&A*, 392, 885
- Corral-Santana J. M., Casares J., Muñoz-Darias T., Rodríguez-Gil P., Shahbaz T., Torres M. A. P., Zurita C., Tyndall A. A., 2013, *Science*, 339, 1048
- Cotton W. D., 2008, *PASP*, 120, 439
- Cumming A., et al. 2001, *ApJ*, 557, 958
- Davis J. E., 2001, *ApJ*, 562, 575
- Degenaar N., Miller J. M., Kennea J., Gehrels N., Reynolds M. T., Wijnands R., 2013, *ApJ*, 769, 155
- Degenaar N., Wijnands R., 2009, *A&A*, 495, 547
- Degenaar N., Wijnands R., 2010, *A&A*, 524, A69
- Degenaar N., Wijnands R., Cackett E. M., Homan J., in't Zand J. J. M., Kuulkers E., Maccarone T. J., van der Klis M., 2012, *A&A*, 545, A49
- Degenaar N., Wijnands R., Miller J. M., 2013, *ApJL*, 767, L31
- Degenaar N., Wijnands R., Reynolds M. T., Miller J. M., Kennea J. A., Gehrels N., 2013, *The Astronomer's Telegram*, 5074, 1
- Del Santo M., Sidoli L., Mereghetti S., Bazzano A., Tarana A., Ubertini P., 2007, *A&A*, 468, L17
- Deufel B., Dullemond C. P., Spruit H. C., 2001, *A&A*, 377, 955
- DeWitt C., Bandyopadhyay R. M., Eikenberry S. S., Blum R., Olsen K., Sellgren K., Sarajedini A., 2010, *ApJ*, 721, 1663
- Dufour F., Kaspi V. M., Gotthelf E. V., Baganoff F. K., Harrison F. A., 2013, *The Astronomer's Telegram*, 5073, 1
- Ekers R. D., van Gorkom J. H., Schwarz U. J., Goss W. M., 1983, *A&A*, 122, 143
- Fruscione A., McDowell J. C., Allen G. E., et al. 2006, in *Society of Photo-Optical Instrumentation Engineers (SPIE) Conference Series* Vol. 6270 of *Society of Photo-Optical Instrumentation Engineers (SPIE) Conference Series*, CIAO: Chandra's data analysis system
- Gallo E., Fender R. P., Miller-Jones J. C. A., Merloni A., Jonker P. G., Heinz S., Maccarone T. J., van der Klis M., 2006, *MNRAS*, 370, 1351
- Gallo E., Miller B. P., Fender R., 2012, *MNRAS*, 423, 590
- Gehrels N., 1986, *ApJ*, 303, 336
- Gierliński M., Done C., Barret D., 2002, *MNRAS*, 331, 141
- Gilfanov M., Revnivtsev M., Sunyaev R., Churazov E., 1998, *A&A*, 338, L83
- Gillessen S., et al. 2012, *Nature*, 481, 51
- Gültekin K., Cackett E. M., Miller J. M., Di Matteo T., Markoff S., Richstone D. O., 2012, *ApJ*, 749, 129
- Harrison F. A., Craig W. W., Christensen F. E., et al. 2013, *ApJ*, 770, 103
- Heinke C., Haggard D., Baganoff F., Ponti G., Rea N., Yusef-Zadeh F., Roberts D., 2013, *The Astronomer's Telegram*, 5095, 1
- Heinke C. O., Cohn H. N., Lugger P. M., 2009, *ApJ*, 692, 584
- Heinke C. O., Rybicki G. B., Narayan R., Grindlay J. E., 2006, *ApJ*, 644, 1090
- Ibragimov A., Poutanen J., 2009, *MNRAS*, 400, 492
- in't Zand J. J. M., Cumming A., van der Sluys M. V., Verbunt F., Pols O. R., 2005, *A&A*, 441, 675
- in't Zand J. J. M., Jonker P. G., Markwardt C. B., 2007, *A&A*, 465, 953
- Israel, G. L. and Stella, L., 1996, *ApJ*, 468, 369
- Jonker P. G., Méndez M., Nelemans G., Wijnands R., van der Klis M., 2003, *MNRAS*, 341, 823
- Kaspi V., et al 2014, *ApJ*, to be submitted
- Kennea J. A., Burrows D. N., Kouveliotou C., et al. 2013, *ApJL*, 770, L24
- Kennea J. A., Wijnands R., Burrows D. N., Nousek J., Gehrels N., 2006a, *The Astronomer's Telegram*, 921, 1
- Kennea J. A., Wijnands R., Burrows D. N., Nousek J., Gehrels N., 2006b, *The Astronomer's Telegram*, 920, 1

- King A. R., Wijnands R., 2006, *MNRAS*, 366, L31
- King I. R., Anderson J., Cool A. M., Piotto G., 1998, *ApJL*, 492, L37
- Lasota J.-P., 2001, *New A Rev.*, 45, 449
- Laycock S., Grindlay J., van den Berg M., Zhao P., Hong J., Koenig X., Schlegel E. M., Persson S. E., 2005, *ApJL*, 634, L53
- Linares M., et al. 2014, *MNRAS*, 438, 251
- Maccarone T. J., Patruno A., 2013, *MNRAS*, 428, 1335
- Masetti N., Landi R., Pretorius M. L., Sguera V., Bird A. J., Perri M., Charles P. A., Kennea J. A., Malizia A., Ubertini P., 2007, *A&A*, 470, 331
- Mauerhan J. C., Munro M. P., Morris M. R., Bauer F. E., Nishiyama S., Nagata T., 2009, *ApJ*, 703, 30
- Migliari S., Fender R. P., 2006, *MNRAS*, 366, 79
- Miller J. M., Cackett E. M., Reis R. C., 2009, *ApJL*, 707, L77
- Moretti A., Campana S., Mineo T., et al. 2005, in Siegmund O. H. W., ed., *SPIE Conference Series Vol. 5898 of SPIE Conf. Ser.*, In-flight calibration of the Swift XRT Point Spread Function. pp 348–356
- Mori K., Gotthelf E. V., Zhang S., et al. 2013, *ApJL*, 770, L23
- Mukai K., Orio M., Della Valle M., 2008, *ApJ*, 677, 1248
- Munro M. P., Baganoff F. K., Bautz M. W., et al., 2003, *ApJ*, 589, 225
- Munro M. P., Lu J. R., Baganoff F. K., Brandt W. N., Garmire G. P., Ghez A. M., Hornstein S. D., Morris M. R., 2005, *ApJ*, 633, 228
- Munro M. P., Pfahl E., Baganoff F. K., Brandt W. N., Ghez A., Lu J., Morris M. R., 2005, *ApJL*, 622, L113
- Oosterbroek T., Parmar A. N., Martin D. D. E., Lammers U., 1997, *A&A*, 327, 2150
- Patruno, A. and Watts, A. L., 2012, *arXiv:1206.2727*
- Plotkin R. M., Gallo E., Jonker P. G., 2013, *ApJ*, 773, 59
- Predehl P., Costantini E., Hasinger G., Tanaka Y., 2003, *Astronomische Nachrichten*, 324, 73
- Predehl P., Schmitt J. H. M. M., 1995, *A&A*, 293, 889
- Rea N., Esposito P., Pons J. A., et al. 2013, *ApJL*, 775, L34
- Reid M. J., 1993, *ARAA*, 31, 345
- Sakano M., Warwick R. S., Decourchelle A., Wang Q. D., 2005, *MNRAS*, 357, 1211
- Shannon R. M., Johnston S., 2013, *MNRAS*, 435, L29
- Sidoli L., Paizis A., Mereghetti S., Götz D., Del Santo M., 2011, *MNRAS*, 415, 2373
- Smak J., 1984, *Acta*, 34, 161
- Stacey W. S., Heinke C. O., Elsner R. F., Edmonds P. D., Weisskopf M. C., Grindlay J. E., 2011, *ApJ*, 732, 46
- Tan J. C., Draine B. T., 2004, *ApJ*, 606, 296
- Titarchuk L., 1994, *ApJ*, 434, 570
- Torii K., et al. 1998, *ApJ*, 508, 854
- Vaughan B. A., et al. 1994, *ApJ*, 435, 362
- van der Klis M., 1989, *Timing Neutron Stars*, 27, Kluwer Academic / Plenum Publishers, New York, NY USA
- Verner D. A., Ferland G. J., Korista K. T., Yakovlev D. G., 1996, *ApJ*, 465, 487
- Walter R., et al. 2004, *The Astronomer's Telegram*, 229, 1
- Wang Z., et al. 2006, *The Astronomer's Telegram*, 935, 1
- Weisskopf M. C., Brinkman B., Canizares C., Garmire G., Murray S., Van Speybroeck L. P., 2002, *PASP*, 114, 1
- Wijnands R., et al. 2006, *A&A*, 449, 1117
- Wilms J., Allen A., McCray R., 2000, *ApJ*, 542, 914
- Wu, Q. and Gu, M., 2008, *ApJ*, 682, 212
- Życki P. T., Done C., Smith D. A., 1999, *MNRAS*, 309, 561

This paper has been typeset from a \TeX / \LaTeX file prepared by the author.